Proceedings of the IASTED International Conference
Solar Energy (SOE 2009)
March 16 - 18, 2009 Phuket, Thailand

INPUT-OUTPUT LINEARIZATION CONTROL OF AN LCL FILTER EMPLOYING A SYMMETRIC GEOMETRY IN GRID-CONNECTED INVERTER APPLICATIONS

Dong-Hyun Ha*, Kui-Jun Lee**, Rae-Young Kim*** and Dong-Seok Hyun**
* Electronics Research Team, Hyundai Rotem Company R&D Center, Korea
** Dept. of Electrical Engineering, Hanyang University, Seoul, Korea
*** Dept. of Electrical and Computer Engineering, Virginia Polytechnic Institute and State University

ABSTRACT
An inductor-capacitor-inductor (LCL) filter is widely adapted in grid-connected inverter applications. In this paper, the harmonic attenuations of the LCL filter are quantitatively analyzed, and then the design optimization of two inductance values, which are related on a cost and a size, is illustrated. Based on the design optimization, the LCL Filter employing a Symmetric Geometry is proposed. Through the equivalent circuit analysis of the proposed LCL filter, the operating characteristics and validity are presented in detail. Furthermore, a state variable decoupling controller by input-output linearization is designed to mitigate the resonance problem. From simulation results, it is seen that the proposed LCL filter and control method have a sufficient attenuation and stability for the grid voltage distortions.

KEY WORDS
LCL filter, Input-output linearization, Modelling, Decoupling, Grid-connected inverter

1. Introduction

Due to increasing demands of interconnection between a distributed power generation system and a existing power grid, a grid-connected inverter has become essential, and thus widely researched to meet various requirements such as low cost, better performance and high reliability. One well-known issue of a grid-connected inverter is to current regulation capability to achieve a desirable sinusoidal current waveform. Various current control methods such as a hysteresis control [1], a proportional-integral (PI) control [2] and predictive control [3] have been proposed to accomplish a better current regulation, and have shown a sufficient regulation capability. However, high frequency harmonic components, which are usually caused from a pulsewidth modulation (PWM) switching, cannot be regulated by the current regulation, and thus a low pass filter is required to attenuate the high frequency harmonics. Two configurations for the low pass filter, called an inductor (L) filter and an inductor-capacitor-inductor (LCL) filter, are widely used. The L filter can be easily implemented due to its simple structure, but larger inductance or higher switching frequency is required to achieve a sufficient attenuation. The LCL filter provides higher harmonic attenuation than that of the L filter, but requires a thoughtful consideration with a current controller design, because of resonance hazards which deteriorate the system stability [4-5]. To avoid the resonance problem, a passive or an active damping technique were proposed by either adding resistor in series with a capacitor or changing a controller design [6-7]. Literatures in [8] showed that system stability depends heavily on feed-back variables of the LCL filter. Moreover, it revels that design of the LCL filter has a large impact on system stability, and needs to be compromising among stability, current regulation capability, efficiency and cost [9].

In an effort to achieve not only a simple structure but also a better current regulation for grid-connected inverter, a novel LCL filter employing a symmetric geometry along with a suitable current control method is proposed. A quantitative analysis of harmonic attenuations of the LCL filter and their minimum values to meet the *total demand distortion* (TDD) in IEEE std. 519-1992 spec. [10] are illustrated. The impacts of the filter parameters, i.e. inductances and capacitance, are evaluated on higher frequency attenuation capability. Based on the evaluation, a symmetric structured inductor, which can reduce size, cost and core loss by combining two inductors into only one magnetic core, is proposed. The realization of the proposed LCL filter is illustrated and the operating characteristics and validity are presented through the equivalent circuit analysis. Furthermore, a state variable decoupling controller by input-output linearization to regulate current in a grid-side inductor is designed in consideration of the resonance problem. Therefore, the verification of sufficient attenuation and resonant mitigation is clearly shown through the simulation results.

2. Proposed LCL Filter

The circuit diagram of the three-phase grid connected inverter with an LCL filter is shown in Fig. 1.

Well-designed current compensator achieves low-order harmonic distortion on the grid current, i2.

However, high frequency current distortions, which could cause from PWM switching or a grid voltage distortion, still exist due to the limit of bandwidth of current compensator. The only way to attenuate the high frequency current distortions is the output filter between inverter and grid, and the LCL filter in Fig. 1 performs this role.

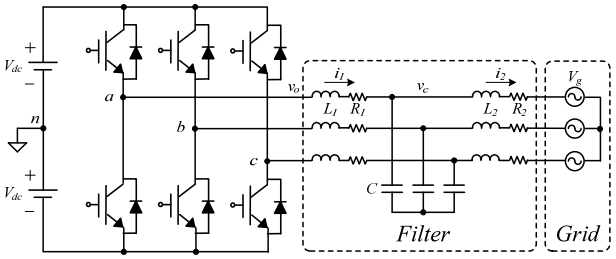

Figure 1. Three-phase grid connected inverter with an LCL filter

Table 1
Design Specifications

Output Power of the Inverter (P_n)	1.5 kW
Grid Line-to-Line Voltage (E_n)	110 Vrms
Grid Frequency (f_o)	60 Hz
DC-Link Voltage ($2V_{dc}$)	300 V
Modulation Index (M)	0.8
Sampling Frequency	20 kHz
Switching Frequency (f_c)	10 kHz

2.1 Filter parameter optimization

To compute the minimum value of LCL filter parameters, the ability of harmonic attenuation is analyzed quantitatively by calculating the TDD. The design specifications used in the analysis are shown in Table I. Since the TDD varies slightly according to the modulation index, this is selected as the expected value (=0.8) at steady state in full load.

Before selection of the optimal inductances, the capacitance is chosen as 10 μF based on (1) in consideration of margin

$$C_f \;<\; 0.05\times\frac{P_n/3}{\omega_o\times\left(E_n/\sqrt{3}\right)^2} \tag{1}$$

where $\omega_o = 2\pi f_o$.

If the capacitance increases, losses and costs can be reduced due to the decrease of inductances. However it has a burden of inrush current and a current caused by low-order harmonics in capacitor. So, the capacitance should be kept as small as possible to restrict low-order current distortions. The remaining two inductances should be selected to satisfy the TDD demand considering the obtained capacitance. For a line voltage between phase leg a and b, the analytical harmonic solution for double-edge naturally sampled PWM of a three-phase inverter is given by (2), where $\omega_c = 2\pi f_c$ and J_n is the Bessel function [11].

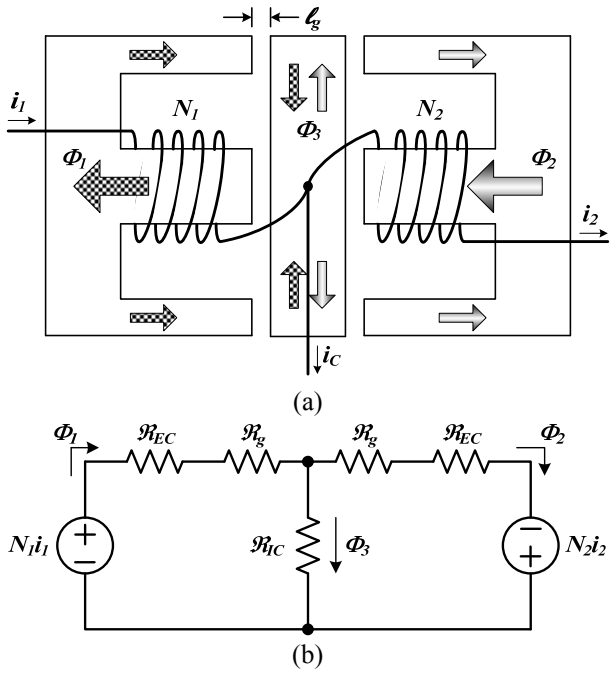

Figure 2. The proposed inductor configuration with symmetric geometry. (a) Physical model. (b) Magnetic circuit model

$$v_{ab}(t) \;=\; \sqrt{3}V_{dc}M\cos\left(\omega_o t+\frac{\pi}{6}\right)+\frac{8V_{dc}}{\pi}\sum_{m=1}^{\infty}\sum_{n=-\infty}^{\infty}\left[\frac{1}{m}J_n\left(m\frac{\pi}{2}M\right)\right.$$
$$\left.\sin\left(\left[m+n\right]\frac{\pi}{2}\right)\sin\left(n\frac{\pi}{3}\right)\times\cos\left(m\omega_c t+n\left[\omega_o t-\frac{\pi}{3}\right]+\frac{\pi}{2}\right)\right],$$
$$\left(m \;=\; 1,2,...,\infty \quad , \quad n \;=\; -\infty,...,-1,0,1,...,\infty\right) \tag{2}$$

$$i_{L_2h} \;=\; \frac{v_o - v_{o1}}{(j\omega)^3 L_1L_2C + j\omega(L_1+L_2)} \tag{3}$$

If it is assumed that there exists no harmonic in V_g, the harmonic current in grid-side inductor (L_2) can be determined by using (2) and the relationship between line-to-line voltage and phase voltage as (3), where v_{o1} is the fundamental component of v_o and $\omega = m\omega_c + n\omega_o$.

The TDD is calculated by varying L_1 and L_2. Consequently, when two inductances are same as $L_1 = L_2 =$ 250 μH, it was identified that the TDD requirement is satisfied and total inductance is minimized. The same calculation was also performed about L filter, and the total 500 μH of LCL filter was 20% of the inductance using only L filter. As a result, higher harmonic attenuation of the LCL filter than that of the L filter was quantitatively proved.

2.2 Configuration of the proposed LCL filter

Based on the preceding results, in this section, the LCL filter employing a symmetric geometry to maximize the advantage of LCL filter is proposed. It is known that the same inductance minimizes the TDD most when the total inductance is constant.

Also, since the structure of an LCL filter has a large impedance of C in the range of fundamental frequency, it can be assumed that the same current flows in L_1 and L_2. In this paper, by utilizing these two factors, the LCL filter through one ferrite EIE core combining two inductors such as Fig. 2(a) is proposed.

In Fig. 2(a), the N_1 and N_2 are the number of turns of conductor flowing currents i_1 and i_2, respectively and the ℓ_g is the length of air gap between E core and I core. By Ampere's law, when a current flows in the winding intersecting the surface, the magnetic filed intensity, H, generates and a magnetic flux is given by $B = \mu_r\mu_0 H$, where $\mu_0 (= 4\pi \times 10^{-7}$ H/m) is the permeability in free space and μ_r is the relative permeability that has the magnitude of 10^3 or 10^4 in case of ferromagnetic material. The Φ_1, Φ_2 and Φ_3 represent the magnetic flux flowing in the corresponding core. The advantages of the proposed LCL filter and operating characteristic are presented in detail through the following circuit modelling.

Fig. 2(b) shows the magnetic circuit model of the physical configuration in Fig. 2(a). The $N_1 i_1$ expressed as voltage source is a magnetomotive force that is generated when the current i_1 flows in the winding of N_1 turns. The $N_2 i_2$ is also modelled similarly as $N_1 i_1$. The $\Re_{EC}$, $\Re_{IC}$ and $\Re_g$ are the reluctance of E core, I core and air gap, respectively and are given by $\Re_{EC} = \Re_{IC} = \ell/\mu_r\mu_0 A_c$, $\Re_g = \ell_g/\mu_0 A_c$, where ℓ is the magnetic path length of corresponding core and A_c is the effective cross section of the core.

The Φ_1, Φ_2 and Φ_3 can be regarded as current when the magnetomotive force is applied to each reluctance. By using a superposition principle, Φ_1 can be represented as the sum of Φ_{11} resulting from $N_1 i_1$ and Φ_{12} resulting from $N_2 i_2$.

$$\begin{aligned}
\Phi_1 &= \Phi_{11} + \Phi_{12} \\
\Phi_{11} &= \frac{N_1 i_1}{\Re_{EC} + \Re_g + [\Re_{IC} /\!/ (\Re_g + \Re_{EC})]} \\
\Phi_{12} &= \frac{N_2 i_2}{\Re_{EC} + \Re_g + [\Re_{IC} /\!/ (\Re_g + \Re_{EC})]} \\
&\quad \times \frac{\Re_{IC}}{(\Re_{EC} + \Re_g) + \Re_{IC}}
\end{aligned} \tag{4}$$

In similar, the Φ_2 and Φ_3 can be calculated as (5) and (6), respectively.

$$\begin{aligned}
\Phi_2 &= \Phi_{21} + \Phi_{22} \\
\Phi_{21} &= \Phi_{11} \times \frac{N_2 i_2}{N_1 i_1}, \Phi_{22} = \Phi_{12} \times \frac{N_1 i_1}{N_2 i_2}
\end{aligned} \tag{5}$$

$$\begin{aligned}
\Phi_3 &= \Phi_{31} + \Phi_{32} \\
\Phi_{31} &= \Phi_{11} \times \frac{\Re_{EC} + \Re_g}{(\Re_{EC} + \Re_g) + \Re_{IC}} \\
\Phi_{32} &= -\Phi_{21} \times \frac{\Re_{EC} + \Re_g}{(\Re_{EC} + \Re_g) + \Re_{IC}}
\end{aligned} \tag{6}$$

It is noted that Φ_3 becomes zero and the magnitude of Φ_1 and Φ_2 becomes equal in ideal condition such that two inductances and two currents are same respectively. Therefore, the loss in I core does not happen due to non-existence of flux, and the width of I core can be practically designed very short.

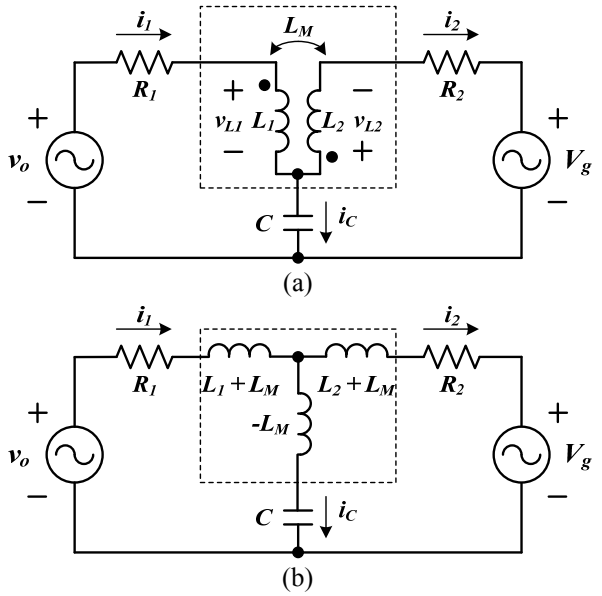

Figure 3. (a) Electrical model with coupling structure. (b) Equivalent electrical model with no coupling structure

Using (4) and (5), the equivalent electrical model of the proposed LCL filter in one phase is shown at Fig. 3(a). From (4), the voltage applied in inductor L_1 can be derived by Faraday's law:

$$\begin{aligned}
v_{L1} &= N_1 \frac{d\Phi_1}{dt} = \frac{N_1^2}{\Re_{EC} + \Re_g + [\Re_{IC} /\!/ (\Re_g + \Re_{EC})]} \frac{di_1}{dt} \\
&+ \frac{N_2^2}{\Re_{EC} + \Re_g + [\Re_{IC} /\!/ (\Re_g + \Re_{EC})]} \times \frac{\Re_{IC}}{(\Re_{EC} + \Re_g) + \Re_{IC}} \frac{di_2}{dt} \\
&= L_{S1} \frac{di_1}{dt} + L_M \frac{di_2}{dt}
\end{aligned} \tag{7}$$

The proportional constants L_{S1} and L_M are defined as self-inductance and mutual inductance, respectively. Since the $\Re_g$ is usually much larger than $\Re_{EC}$ and $\Re_{IC}$, the L_{S1} and L_M can be approximated as

$$L_{S1} \approx \frac{N_1^2}{\Re_g}, \quad L_M \approx \frac{N_2^2 \Re_{IC}}{\Re_g^2} \tag{8}$$

Also, v_{L2} can be presented as

$$v_{L2} = L_{S2}\frac{di_2}{dt} + L_M\frac{di_1}{dt} \tag{9}$$

and then Fig. 3(a) can be converted to the equivalent electrical model in Fig. 3(b), where $L_1 + L_M = L_{s1}$, $L_2 + L_M = L_{s2}$.

Since this form combines two discrete inductors having EI core, it has advantages of reduction in volume and weight. Also, during combining procedure, one of two I cores can be removed, and even the width of applied I core can be very short practically. However the effect of newly occurred mutual inductance should be carefully inspected. This is described in next modelling part.

3. Modelling of Grid-connected Inverter

3.1 Modelling in rotating *dq* frame

The system equations in stationary *abc* frame using the proposed LCL filter including the mutual inductance of Fig 3(b) are as follows:

$$\begin{aligned}
\frac{d}{dt}i_{1abc} &= \frac{1}{L_1}v_{oabc} - \frac{1}{L_1}v_{cabc} - \frac{L_M}{L_1}\frac{d}{dt}i_{2abc} \\
\frac{d}{dt}v_{cabc} &= \frac{1}{C}i_{1abc} - \frac{1}{C}i_{2abc} \\
\frac{d}{dt}i_{2abc} &= -\frac{L_M}{L_2}\frac{d}{dt}i_{1abc} + \frac{1}{L_2}v_{cabc} - \frac{1}{L_2}v_{gabc}
\end{aligned} \tag{10}$$

Assuming that the three phase systems are balanced for the simplicity of analysis, it can be converted to (11) in synchronous *dq* frame without zero-sequence component.

$$\begin{aligned}
\frac{d}{dt}i_{1dq} &= \frac{1}{L_1}v_{odq} + j\omega\cdot i_{1dq} - \frac{1}{L_1}v_{cdq} - \frac{L_M}{L_1}\frac{d}{dt}i_{2dq} + \frac{L_M}{L_1}j\omega\cdot i_{2dq} \\
\frac{d}{dt}v_{cdq} &= \frac{1}{C}i_{1dq} + j\omega\cdot v_{cdq} - \frac{1}{C}i_{2dq} \\
\frac{d}{dt}i_{2dq} &= -\frac{L_M}{L_2}\frac{d}{dt}i_{1dq} + \frac{L_M}{L_2}j\omega\cdot i_{1dq} + \frac{1}{L_2}v_{cdq} + j\omega\cdot i_{2dq} - \frac{1}{L_2}v_{gdq}
\end{aligned} \tag{11}$$

The additional coupling term from L_M as well as the ordinary coupling elements due to L_1, L_2, C in LCL filter occurs, and it results in very complex nonlinear structure.

3.2 Effect of mutual inductance

The characteristic of proposed LCL filter is the mutual inductance, compared with the conventional LCL filter. Therefore, to understand the effect of the mutual inductance on systems and to design the relevant controller in next section, it requires the analysis about this.

If the N_1 equals to N_2 from (8), the $L_M = (\mathcal{R}_{IC}/\mathcal{R}_g)L_s = (l/u_r l_g)L_s$ is obtained. So, it can be stated that the mutual inductance has usually the maximum 10% of the self-inductance. However, it is does not nearly affect the overall system response. Therefore, the mutual inductance in the proposed LCL filter can be neglected, and then the proposed LCL filter can replace the conventional discrete LCL filter without additional compensation.

4. Control Strategy

From (11), the *dq* model of LCL filter is nonlinear system including many coupling elements and resonance. Thus, to decouple and linearize the model and for active damping to suppress the resonance, an input-output linearization method is applied. This method provides the direct relation between output and input variables, and applies the linearization scheme. Furthermore, unlike a small signal model approach, it is possible to control with same dynamic performance regardless of dc operating point.

4.1 Input-output linearization

This method differentiates the output variables continuously until more than one input variable appears. Afterward, the input variables are designed to linearize and decouple the system. From the preceding results, the mutual inductance can be neglected, so that the mutual inductance is assumed to be zero in order to simplify the analysis.

By expanding the *dq* model in (11) into its components yields

$$\begin{aligned}
\frac{d}{dt}i_{1d} &= \frac{1}{L_1}v_{od} + \omega\cdot i_{1q} - \frac{1}{L_1}v_{cd} \\
\frac{d}{dt}i_{1q} &= \frac{1}{L_1}v_{oq} - \omega\cdot i_{1d} - \frac{1}{L_1}v_{cq} \\
\frac{d}{dt}v_{cd} &= \frac{1}{C}i_{1d} + \omega\cdot v_{cq} - \frac{1}{C}i_{2d} \\
\frac{d}{dt}v_{cq} &= \frac{1}{C}i_{1q} - \omega\cdot v_{cd} - \frac{1}{C}i_{2q} \\
\frac{d}{dt}i_{2d} &= \frac{1}{L_2}v_{cd} + \omega\cdot i_{2q} - \frac{1}{L_2}v_{gd} \\
\frac{d}{dt}i_{2q} &= \frac{1}{L_2}v_{cq} - \omega\cdot i_{2d} - \frac{1}{L_2}v_{gq}
\end{aligned} \tag{12}$$

the resulting model (12) does not have direct relation between output variables (i_{2d}, i_{2q}) and input variables (v_{od}, v_{oq}) respectively. Therefore, if $(d/dt)i_{2d}$ is differentiated, yields

$$\frac{d^2}{dt^2}i_{2d} = \frac{1}{L_2C}i_{1d} + \frac{2\omega}{L_2}v_{cq} + \left(\frac{-1}{L_2C} - \omega^2\right)i_{2d} - \frac{\omega}{L_2}v_{gq} - \frac{1}{L_2}\frac{d}{dt}v_{gd} \tag{13}$$

Because it does not contain the input variable, it is differentiated again, yields

$$\frac{d^3}{dt^3}i_{2d}=\left(\frac{1}{L_1L_2C}\right)v_{od}+\frac{3\omega}{L_2C}i_{1q}+\left(\frac{-1}{L_1L_2C}-\frac{3\omega^2}{L_2}-\frac{1}{L_2{}^2C}\right)v_{cd}$$
$$+\left(\frac{-3\omega}{L_2C}-\omega^3\right)i_{2q}+\left(\frac{1}{L_2{}^2C}+\frac{\omega^2}{L_2}\right)v_{gd}-\frac{\omega}{L_2}\frac{d}{dt}v_{gq}-\frac{1}{L_2}\frac{d^2}{dt^2}v_{gd} \tag{14}$$

Since (14) contains the input variable, the differentiation is stopped, and the same procedure is applied to i_{2q}, which yields

$$\frac{d^3}{dt^3}i_{2q}=\left(\frac{1}{L_1L_2C}\right)v_{oq}-\frac{3\omega}{L_2C}i_{1d}+\left(\frac{-1}{L_1L_2C}-\frac{3\omega^2}{L_2}-\frac{1}{L_2{}^2C}\right)v_{cq}$$
$$+\left(\frac{3\omega}{L_2C}+\omega^3\right)i_{2d}+\left(\frac{1}{L_2{}^2C}+\frac{\omega^2}{L_2}\right)v_{gq}+\frac{\omega}{L_2}\frac{d}{dt}v_{gd}-\frac{1}{L_2}\frac{d^2}{dt^2}v_{gq} \tag{15}$$

Equations (14) and (15) can be expressed in a matrix form as

$$X(t)=A(t)\cdot d_{dq}+B(t) \tag{16}$$

where

$$X(t)=\left[\left(d^3/dt^3\right)i_{2d}\quad\left(d^3/dt^3\right)i_{2q}\right],\quad d_{dq}=v_{odq}/V_{dc},$$
$$A(t)=\frac{1}{L_1L_2C},$$
$$B(t)=\begin{bmatrix}\dfrac{3\omega}{L_2C}i_{1q}+\left(\dfrac{-1}{L_1L_2C}-\dfrac{3\omega^2}{L_2}-\dfrac{1}{L_2{}^2C}\right)v_{cd}\\ -\dfrac{3\omega}{L_2C}i_{1d}+\left(\dfrac{-1}{L_1L_2C}-\dfrac{3\omega^2}{L_2}-\dfrac{1}{L_2{}^2C}\right)v_{cq}\end{bmatrix}$$
$$+\begin{bmatrix}\left(\dfrac{-3\omega}{L_2C}-\omega^3\right)i_{2q}+\left(\dfrac{1}{L_2{}^2C}+\dfrac{\omega^2}{L_2}\right)v_{gd}-\dfrac{\omega}{L_2}\dfrac{d}{dt}v_{gq}-\dfrac{1}{L_2}\dfrac{d^2}{dt^2}v_{gd}\\ \left(\dfrac{3\omega}{L_2C}+\omega^3\right)i_{2d}+\left(\dfrac{1}{L_2{}^2C}+\dfrac{\omega^2}{L_2}\right)v_{gq}+\dfrac{\omega}{L_2}\dfrac{d}{dt}v_{gd}-\dfrac{1}{L_2}\dfrac{d^2}{dt^2}v_{gq}\end{bmatrix}$$

The second step of the input-output linearization is to express $X(t)$ as linear and decoupled form:

$$X(t)=D\cdot u_{dq}+F(t) \tag{17}$$

where

$$D=k_3$$
$$F(t)=\begin{bmatrix}-k_1\dfrac{d^2}{dt^2}i_{2d}-k_2\dfrac{d}{dt}i_{2d}-k_3i_{2d}\\ -k_1\dfrac{d^2}{dt^2}i_{2q}-k_2\dfrac{d}{dt}i_{2q}-k_3i_{2q}\end{bmatrix}$$

The u_{dq} is a new input variable, and k_1, k_2 and k_3 are arbitrary gains for pole placement. The input transformation is achieved by using (16) and (17) as

$$d_{dq}=A^{-1}(t)\cdot\left(D\cdot u_{dq}+F(t)-B(t)\right) \tag{18}$$

Although the existence of (18) depends on the existence of A^{-1}, there is no problem because A is always the positive constant. To calculate the $B(t)$ in (18), it requires the differential of grid voltage. However, since the frequency of grid voltage is much smaller than the sampling frequency, it can be assumed that the grid voltage is constant during one sampling time, and then the zero is applied. Furthermore, the differential term in $F(t)$ can be obtained by using only state variables of (13)-(15), so that the differential of currents are not required. Besides, the voltage sensors can be reduced by using similar grid voltage in place of capacitor voltage. Therefore, it is possible to minimize the effect of the noise.

The last step is to identify the stability of internal dynamics. Since two output variables (i_{2d}, i_{2q}) are differentiated three times respectively to obtain the relation between input and output variables, the total relative degree of the system is six [12]. However, since the dimension of the system is six, the internal dynamics become zero. Thus, in this case, both system stability and output tracking of reference value are achieved easily regardless of the stability of internal dynamics.

4.2 Dynamic response optimization

Since the system of (17) is linear, it is converted by Laplace transform and written as

$$\frac{I_{2d}(s)}{U_d(s)}=\frac{I_{2q}(s)}{U_q(s)}=\frac{k_3}{s^3+k_1s^2+k_2s+k_3} \tag{19}$$

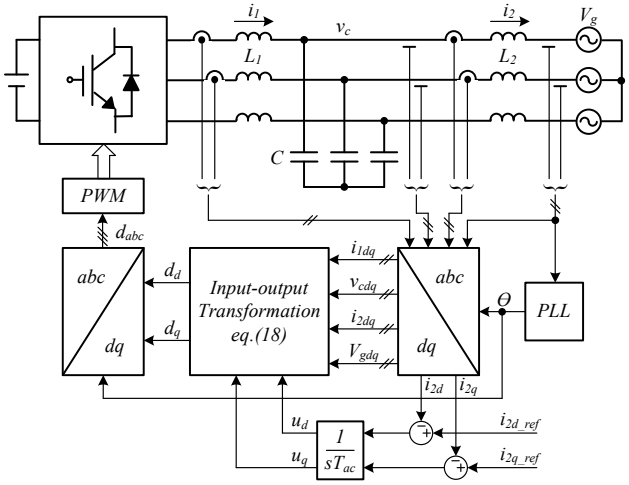

Figure 4. Block diagram of current control

where $I_{2d}(s)$, $I_{2q}(s)$, $U_d(s)$ and $U_q(s)$ are the Laplace transform of i_{2d}, i_{2q}, u_d and u_q, respectively. When the parameter values are exactly estimated and the input transformation (18) is accurately achieved, the (19) forces the steady state error to be zero. However, since the exact estimation of parameters (L_1, L_2, C) is not possible, the

integrator in inserted to satisfy zero of steady state error, even for parameters errors.

If the feedback loop is formed by adding the integrator ($1/sT_{ac}$), the closed-loop transfer function of current become

$$\frac{I_{2d}(s)}{I_{2d\_ref}(s)} = \frac{I_{2q}(s)}{I_{2q\_ref}(s)} = \frac{k_3 / T_{ac}}{s^4 + k_1 s^3 + k_2 s^2 + k_3 s + k_3 / T_{ac}} \quad (20)$$

and the overall block diagram of current control is shown at Fig. 4.

Based on itae-criterion [13], the optimum third-order transfer function is

$$\frac{(7.54/t_s)^4}{s^4 + 2.1(7.54/t_s)s^3 + 3.4(7.54/t_s)^2 s^2 + 2.7(7.54/t_s)^3 s + (7.54/t_s)^4} \quad (21)$$

where t_s is the settling time to reach within 2% band of steady state.

If the desired settling time is set as t_{s_ac} and (20) is matched to (21), k_1, k_2, k_3 and T_{ac} are obtained as

$$k_1 = 2.1\frac{7.54}{t_{s\_ac}}, k_2 = 3.4\left(\frac{7.54}{t_{s\_ac}}\right)^2, k_3 = 2.7\left(\frac{7.54}{t_{s\_ac}}\right)^3, \quad (22)$$

$$T_{ac} = 2.7\frac{t_{s\_ac}}{7.54}$$

5. Simulation Results

Fig. 5 and Fig. 6 show the simulation results of inductor currents and grid voltage using the conventional LCL filter and the proposed LCL filter respectively. The proposed LCL filter is assumed to have 10% mutual inductance of self-inductance.

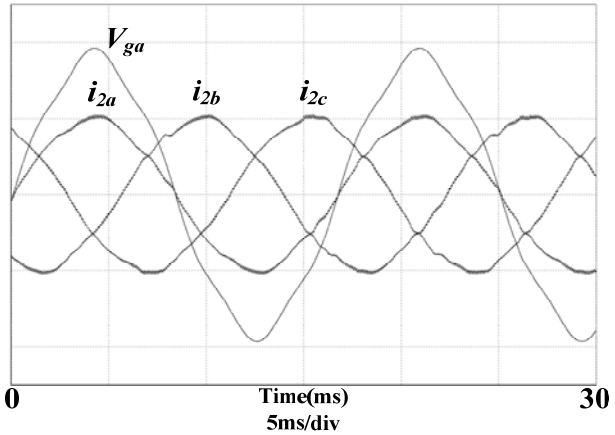

Figure 5. Inductor currents and grid voltage waveform using the conventional LCL filter ($L_1 = L_2 = 250\ \mu$H and $C = 10\ \mu$F) with 5% fifth and 3% seventh grid voltage harmonic. Time: 5 ms/div., i_{2a}, i_{2b}, i_{2c} : 10 A/div., V_{ga}: 50 V/div

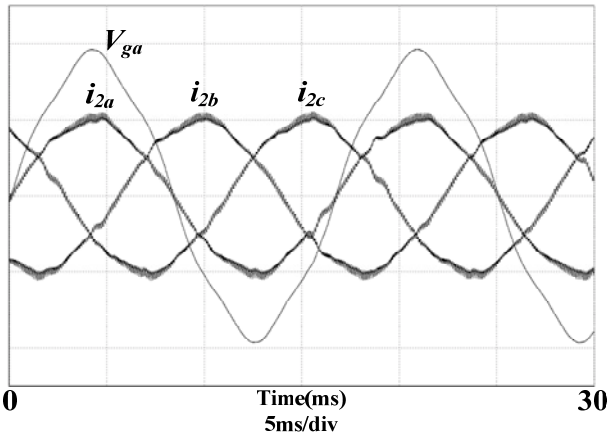

Figure 6. Inductor currents and grid voltage waveform using the proposed LCL filter ($L_1 = L_2 = 250\ \mu$H and $C = 10\ \mu$F) with 5% fifth and 3% seventh grid voltage harmonic. Time: 5 ms/div., i_{2a}, i_{2b}, i_{2c} : 10 A/div., V_{ga}: 50 V/div

The simulations are performed at the same condition shown in Table I except for the modulation index, and also, the grid voltage is assumed to have 5% fifth and 3% seventh harmonic. Furthermore, the same controller proposed in this paper is applied and the controller gains are chosen as k_1 = 1.979e4, k_2 = 3.02e8, k_3 = 2.261e12, T_{ac} = 2.865e-4 to achieve a 0.8 ms settling time. It can be known that the currents are well regulated, and the similar waveforms are achieved.

6. Conclusion

Through the superior harmonic reduction with two same inductances in an LCL filter, the LCL filter employing a symmetric geometry is proposed and the characteristics and performance of the LCL are presented by using the equivalent circuit modelling. The proposed LCL filter integrates two inductors into one EIE core structure, so that the volume and weight can be reduced, and also it is identified that the effect of mutual inductance can be ignored due to very low coupling coefficient from placing a relevant air gap between E core and I core. Therefore, it can replace easily the conventional LCL form. Furthermore, to regulate the grid current with linear and decoupled form, an input-output linearization method is applied. The validity of the proposed LCL filter is verified through the simulation results with the designed current controller.

References

[1] D. M. Brod and D. W. Novotny, "Current control of VSI_PWM inverters," *IEEE Trans. Ind. Appl.*, *vol. IA-21*, no. 4, pp. 562-570, Nov. 1985.

[2] T. M. Rowan and R. J. Kerkman, "A new synchronous current regulator and an analysis of current-regulated PWM inverters," *IEEE Trans. Ind. Appl.*,

vol. IA-22, no. 4, pp. 678-690, Jul/Aug. 1986.
[3] D. G. Holmes and D. A. Martin, "Implementation of a direct digital predictive current controller for single and three phase voltage source inverters," in *Proc. Annu. Meeting Industry Appl. Society*, Oct. 1996, pp. 906-913.
[4] E. Twining and D. G. Holmes, "Grid current regulation of a three-phase voltage source inverter with an LCL input filter," *IEEE Trans. Power Electron.*, *vol. 18*, no. 3, pp. 888-895, May 2003.
[5] E. Wu and P. W. Lehn, "Digital current control of a voltage source converter with active damping of LCL resonance," *IEEE Trans. Power Electron.*, *vol. 21*, no. 5, pp. 1364-1373, Sep. 2006.
[6] M. Liserre, A. Dell'Aquila, and F. Blaabjerg, "Stability improvements of an LCL-filter based three-phase active rectifier," in *Proc. Power Electron. Specialists Conf.*, Cairns, Australia, Jun. 2002, pp. 1195–1201.
[7] M. Liserre, A. Dell'Aquila, and F. Blaabjerg, "Genetic algorithm-based design of the active damping for an LCL-filter three-phase active rectifier," *IEEE Trans. Power Electron.*, *vol. 19*, pp. 76–86, Jan. 2004.
[8] T. Abeyasekera, C. M. Johnson, D. J. Atkinson, and M. Armstrong, "Suppression of line voltage related distortion in current controlled grid connected inverters," *IEEE Trans. Power Electron.*, *vol. 20*, pp. 1393-1401, Nov. 2005.
[9] T. C. Wang, Z. H. Ye, G. Sinha, and X. M. Yuan, "Output filter design for a grid-interconnected three-phase inverter," in *Proc. Power Electron. Specialists Conf.*, Acapulco, Mexico, Jun. 2003, pp. 779-782.
[10] IEEE std. 519-1992 – IEEE Recommended Practices and Requirements for Harmonic control in Electrical Power Systems – IEEE Power Engineering Society / Industry Applications Society.
[11] D. G. Holmes, T. A. Lipo, *Pulse Width Modulation for Power Converters – Principle and practice*, IEEE Press, 2003.
[12] J. Slotine and W. Li, *Applied Nonlinear Control*. Englewood Cliffs, NJ: Prentice-Hall, 1991.
[13] R. Dorf, *Modern Control Systems*, Reading, MA: Addison-Wesley, 1992.